Structural Transition of $RhSb_3$ under High Pressures

Satoshi Takanashi,[1] Takumi Hasegawa,[1,*] Norio Ogita,[1] and Masayuki Udagawa[1,2]

[1] *Graduate School of Integrated Arts and Sciences, Hiroshima University, Higashi-Hiroshima, 739-8521, Japan*

[2] *Institute for Advanced Material Research, Hiroshima University, Higashi-Hiroshima, 739-8530, Japan*

(Received April 12, 2010)

Structures of $RhSb_3$ under high pressures up to 95 GPa have been investigated by first-principles calculations. The calculated phonon dispersion curves with space group $Im\bar{3}$ show unstable triply degenerated modes at the H point ($\mathbf{q}$ = (1/2, 1/2, 1/2)) above 53 GPa. According to Landau theory, the possible space groups as distorted structures at high pressures are Pnnm and $R\bar{3}$. The obtained structural distortions are not self-insertion reaction but are collapse of the cage structure. By comparing their Gibbs free energies with that of undistorted structure $Im\bar{3}$, it is found that the first-order structural transition to the Pnnm symmetry occurs at around 22 GPa, which is close to the observed pressure in the experiments.

PACS numbers: 61.50.Ks, 63.20.dk, 63.70.+h

I. INTRODUCTION

Skutterudite compounds have a chemical formula TX_3, where T = Co, Rh, and Ir and X = P, As, and Sb. A remarkable feature of the skutterudite compounds is that there is a large space surrounded by twelve X atoms. This cage structure can include an atom as a guest. Since one cage exists per four formula units, the compounds with fully occupied cages have a chemical formula AT_4X_{12}, which is called filled-skutterudite. The skutterudite compounds can maintain the cage structure without guest atoms. Therefore, the cage can include rather small guest atom without structural distortion. Since such a small guest vibrates quite largely, the large amplitude vibrations are expected to cause exotic phenomena, such as large anharmonicity [1–5], small lattice thermal conductivity [6, 7], and heavy-fermion electronic state [8, 9]. On the other hand, stability of the cage structures has been examined under high pressures [10–12].

Phase transition under pressures is discussed using the Gibbs free energy, $G(T, P)$. G is written as $G = F + PV$, where F is the Helmholtz free energy, P is pressure, and V is volume. From the Gibbs free energy, it can be concluded that a high-pressure phase generally has higher F and lower V when compared to the low-pressure phase. Kraemer *et al.* [10] have reported that $CoSb_3$ shows a structural distortion at around 20 GPa and also that the distorted structure has a larger volume than it did before the distortion. This strange observation has been explained as a result of a self-insertion reaction. The self-insertion reaction is a reaction in which an Sb atom moves into the cage constructed by Sb

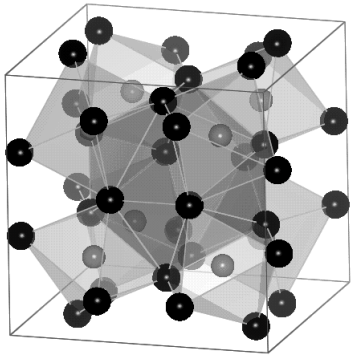

FIG. 1: Skutterudite structure. Gray sphere and black sphere are Rh and Sb, respectively. The dark polyhedron at the center of the unit cell is the cage structure.

atoms. Therefore, they have concluded that unfilled-skutterudite $CoSb_3$ becomes partially filled skutterudite $Sb_xCo_4Sb_{12-x}$ under high pressures. Similar volume expansion has been observed for $RhSb_3$ and $IrSb_3$ under pressures of around 20–30 GPa [13].

The self-insertion reaction will lead to volume expansion if we assume the cage structure is maintained. However, since it makes many defects in the cages, the resultant volume expansion and conservation of the cage structure are not clear. Therefore, to examine the self-insertion reaction and other possibilities, structures of unfilled-skutterudites under high pressures have been investigated using first-principles calculation.

II. CALCULATION

All calculations have been performed using the ABINIT code [14–16], which is based on *ab-initio* pseudopotentials and a plane-wave basis set in the framework of the density functional theory. It relies on an efficient Fast Fourier Transform algorithm [17] for the conversion of wavefunctions between real and reciprocal space, on the adaptation to a fixed potential of the band-by-band conjugate gradient method [18], and on a potential-based conjugate-gradient algorithm for the determination of the self-consistent potential [19]. The local-density approximation has been adopted for the exchange-correlation energy, which is parameterized by Perdew and Wang [20]. The Troullier-Martines type pseudopotentials [21] have been generated by FHI98PP code [22]. For Rh atom, 5s, 5p, and 4d electrons are treated as covalent electrons, and their cutoff radii are set to 1.06, 1.22, and 1.43 Å, respectively. For Sb atom, 5s and 5p are covalent, and their cutoff radii are 1.18 and 1.24 Å, respectively. The cutoff energy of the plane-wave basis set is 40 Ry, where 1 Ry = 13.606 eV. For integration in the reciprocal space, $4 \times 4 \times 4$ Monkhorst-Pack grid [23] has been employed.

The computations of the responses to atomic displacements and electric fields have been performed within the density functional perturbation theory [24]. The interatomic

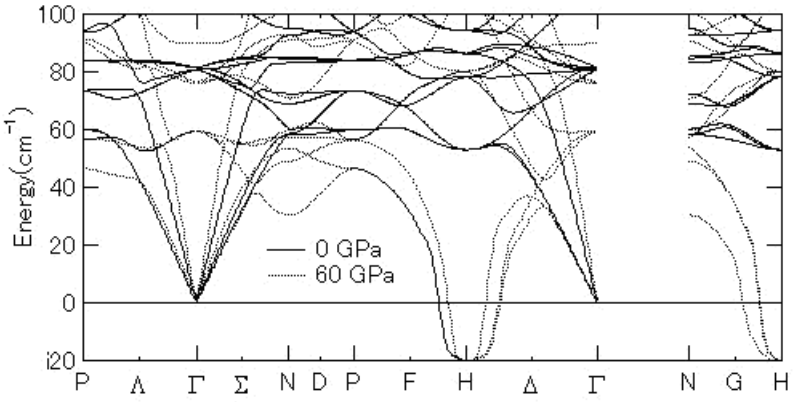

FIG. 2: Phonon dispersion curves of $RhSb_3$ with $Im\bar{3}$ structure below 100 cm^{-1} at 0 GPa and 60 GPa. Imaginary energy below 0 cm^{-1} means unstable.

force constants have been determined by the Fourier interpolation method based on $4 \times 4 \times 4$ grid of the cubic Bravais cell in the reciprocal space. Then, the phonon dispersion curves have been calculated using the interatomic force constants [25]. For the response calculations, a $2 \times 2 \times 2$ Monkhorst-Pack grid has been adapted, where we had confirmed that the differences of phonon frequencies at 0 GPa from those obtained with the $6 \times 6 \times 6$ Monkhorst-Pack grid is lower than 5 cm^{-1}.

III. RESULT AND DISCUSSION

Figure 1 shows unfilled skutterudite structure of $RhSb_3$ with space group $Im\bar{3}$. It consists of vertex-shared $RhSb_6$ octahedra. Therefore, it is obtained from an ReO_3 structure by rotating octahedra. As a result of the rotation, the skutterudite structure has a large space surrounded by twelve Sb atoms in the unit cell. This structure constructed by twelve Sb atoms (dark polyhedron in Fig. 1) is called the cage. The skutterudite structure has three parameters: lattice constant a, and Sb position parameters (0, y, z). These parameters are obtained by the optimization of the structure to minimize electronic energy under pressures. We can calculate from the obtained lattice parameters (shown in Fig. 4) the bulk modulus $B_0 = 111$ GPa and the pressure derivative of bulk modulus $B_0' = 4.44$, using the Birch-Murnaghan equation of state [26]. These are reasonable values, since the experimental results reported that B_0 and B_0' are 93 GPa and 4.0 for $CoSb_3$ [11], and 136 GPa and 4.8 for $IrSb_3$ [12].

Using the optimized structures, phonon dispersion curves have been calculated under pressures. Figure 2 shows the phonon dispersion curves at 0 GPa and 60 GPa. Unstable modes with pure imaginary energy can be found at the H point (wavevector **q**

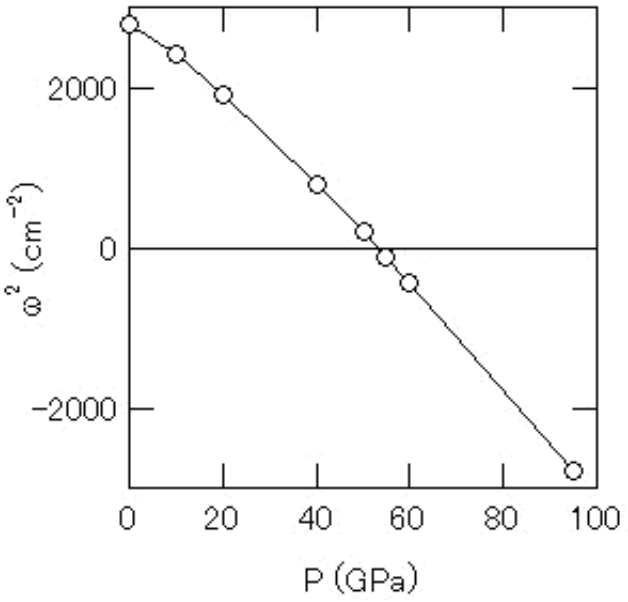

FIG. 3: Pressure dependence of square energy of unstable H_7 mode

$= (1/2, 1/2, 1/2)$ in the primitive cell and (1, 0, 0) in the conventional cell. Hereafter, we will use the primitive cell coordinate.) at 60 GPa. Pressure dependence of square frequency ω^2 of the unstable modes is shown in Fig. 3. It is found that the modes become unstable at 53 GPa. Under pressures higher than 53 GPa, distorted structures can be obtained by optimizing the structures, because any small displacement of these unstable modes decreases the total energy.

TABLE I: Character table at H point in $Im\bar{3}$ space group.

	E	$3C_2$	$8C_3$	I	3m	$8S_6$
H_1	1	1	1	1	1	1
H_2	1	1	1	-1	-1	-1
H_{35}	2	2	-1	2	2	-1
H_{46}	2	2	-1	-2	-2	1
H_7	3	-1	0	3	-1	0
H_8	4	-1	0	-3	1	0

Before discussing distorted structure, we consider the symmetric property of the unstable modes and Landau free energy analysis under pressures. We show the character table at the H point in Table I. The H point has the same symmetry as that of the Γ point. Therefore, the character table is similar to that of the Γ point, i.e., that of the point group $m\bar{3}$. However, we cannot distinct even and odd parity by inversion symmetries at the H

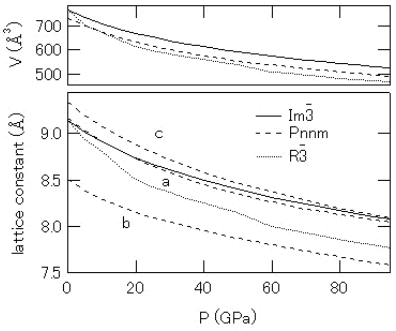

FIG. 4: Lattice constants and volumes of Bravais cell in three structures under pressures.

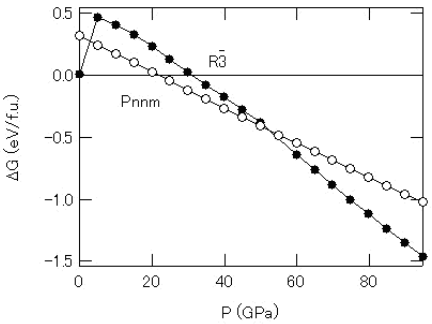

FIG. 5: Differences of Gibbs free energy from Im$\bar{3}$ structure

point. For example, H_7 modes have characters similar to those of the T_g modes at the Γ point, though H_7 modes are symmetric by the inversion at $(0,0,0)$ and are anti-symmetric by the inversion at $(0.25,0.25,0.25)$. Thus, we can say that modes at the H point are always symmetric for a half of inversion centers. In Table I, we show only the symmetric operations at the origin.

To expand the free energy, we need all degeneracy for the unstable modes in the Brillouin zone. The unstable modes are triply degenerated H_7 modes at the H point. Since there is only one H point in the Brillouin zone, three modes of the H_7 modes are considered as the order parameters. They are written as u_x, u_y, and u_z. According to Landau theory, free energy F can be expanded up to the fourth order terms of the order parameters,

$$F = a(u_x^2 + u_y^2 + u_z^2) + b(u_x^4 + u_y^4 + u_z^4) + c(u_x^2u_y^2 + u_y^2u_z^2 + u_z^2u_x^2) \quad (1)$$

To ensure structural stability, $b+c > 0$ and $2b+c > 0$ must be satisfied. For P > 53 GPa, the coefficient a becomes negative. Then, we can obtain two solutions with non-zero u values by minimizing F. For $2b < c$, we obtain $u_x^2 = -a/2b, u_y^2 = u_z^2 = 0$, and $F = -a2/4b$. The structure becomes an orthorhombic one with Pnnm space group. For $2b > c$, we obtain $u_x^2 = u_y^2 = u_z^2 = -a/2(b+c)$, and $F = -3a2/4(b+c)$. Then, the structure becomes a rhombohedral one with R$\bar{3}$ space group. If the parameters satisfy $2b = c$ or are very close to the relation, sixth-order terms will be important, and we can obtain third solution with $u_x^2 = u_y^2$ and $u_z^2 = 0$. However, we do not discuss this case in this paper.

Some comments about the analysis should be noted. The experiment has indicated first-order transition at around 20 GPa. It is lower than 53 GPa, where the second-order transition is expected due to unstable H_7 mode from the calculated result. This means that the expansion of F must be extended up to the sixth-order terms. However, we can estimate only the second-order coefficient a from the present calculations and the sixth-order terms are not important for the discussion of distorted structures. Therefore, we used the fourth-order expansion eq. (1) to discuss possible structures, and the Gibbs free energies under pressures were examined to investigate the first-order transition instead of the Landau analysis as shown later.

TABLE II: Structural parameters for $Im\bar{3}$ and Pnnm structures at 0 GPa and for $R\bar{3}$ structures at 5 GPa.

$Im\bar{3}$		Pnnm		$R\bar{3}$	
$a = 9.148$ Å		$a = 9.172$ Å,$b = 8.502$ Å,$c = 9.341$ Å		$a = 8.933$ Å,$\alpha = 84.117°$	
Rh	$(0.25, 0.25, 0.25)$	Rh	$(0.1853, 0.1608, 0.2559)$	Rh(1)	$(0.1938, 0.1938, 0.1938)$
				Rh(2)	$(0.6760, 0.2528, 0.2800)$
Sb	$(0, 0.1544, 0.3398)$	Sb(1)	$(0.06159, 0.1554, 0)$	Sb(1)	$(0.9345, 0.3143, 0.1275)$
		Sb(2)	$(0.1673, 0.6145, 0)$	Sb(2)	$(0.0052, 0.6279, 0.1874)$
		Sb(3)	$(0.9017, 0.1446, 0.3402)$	Sb(3)	$(0.5576, 0.9067, 0.7061)$
		Sb(4)	$(0.3527, 0.9442, 0.1515)$	Sb(4)	$(0.5318, 0.2147, 0.5680)$

The unstable modes have the wavevector $\mathbf{q}= (1/2, 1/2, 1/2)$. Freezing of the mode causes the unit cell doubling, i.e. the unit cell becomes a simple cell from the body-centered cell. According to this consideration, we have optimized the structure at 60 GPa with the doubled unit cell without any symmetric restriction. The obtained structure satisfies the Pnnm space group, which agrees with the abovementioned analysis. Moreover, we can obtain another structure with $R\bar{3}$ space group, where the structure is optimized under a condition to satisfy the $R\bar{3}$ space group. Therefore, we obtain three structures with different space groups, i.e., undistorted $Im\bar{3}$, and distorted Pnnm, and $R\bar{3}$. From now on, we discern these structures by their space groups. The optimized structural parameters for $Im\bar{3}$ and Pnnm at 0 GPa and for $R\bar{3}$ at 5 GPa are shown in Table II. The $R\bar{3}$ structure restores $Im\bar{3}$ symmetry at 0 GPa, while the Pnnm structure remains at 0 GPa. It is found that structural distortions are very large for both structures. However, the distortion is not a self-insertion reaction but is a collapse of the cage structure. As the result of the collapse, coordination number of Rh in Pnnm and Rh(2) in $R\bar{3}$ increases from 6 to 7. Thus, both distorted structures become metallic.

Figure 4 shows pressure dependences of the lattice parameters and volumes of the unit cell for three structures. It is found that the volume is reduced for both structures because of the collapse of the cage structure. Gibbs free energies G at 0 K for the three structures can be estimated by $G = E + PV$, where E is the total energy obtained from electronic structure calculations. The differences $\Delta G = G - G_0$ where G_0 is the Gibbs free energy of the $Im\bar{3}$ structure is shown in Fig. 5 for the Pnnm and $R\bar{3}$ structures. It is noticed that both structures have larger E and smaller V than $Im\bar{3}$ does. From the obtained G, it is concluded that a first-order transition from $Im\bar{3}$ to Pnnm occurs at around 22 GPa and second first-order transition from Pnnm to $R\bar{3}$ happens around 55 GPa at a sufficiently high temperature. It is worth noting that the transition pressure from $Im\bar{3}$ to Pnnm is close to the experimental value of ∼20 GPa [10, 13]. This suggests that the distorted structure observed in the experiments is Pnnm.

Another evidence of Pnnm structure is that the lattice parameter c is larger than a of $Im\bar{3}$. In the study of $CoSb_3$ distortion [10], line shapes of the $(3, 0, 1)$ and $(3, 2, 1)$ Bragg peaks have been studied in detail. (For the indices of Bragg peaks, the coordinate of the

conventional cell is used.) Each of the peaks consists of two peaks: a sharp one is from the undistorted $Im\bar{3}$ structure and a broad one from a distorted structure. The peak top of the broad one has been found at lower diffraction angle than that of the sharp one. This leads the volume expansion if we assume no symmetric change. We will consider the $(3, 0, 1)$ Bragg peak. In Pnnm structure, the Bragg peak splits into six peaks. From the structure shown in Table II, four peaks of $(1, 0, 3), (0, 1, 3), (3, 0, 1)$, and $(3, 1, 0)$ are observed at diffraction angles below the $(3, 0, 1)$ Bragg peak of $Im\bar{3}$ structure. If the Bragg peaks from a distorted structure are broad, these four peaks become one broad peak and its diffraction angle is lower than that of $(3, 0, 1)$ of $Im\bar{3}$. This is consistent with the experimental observation. In addition, around $(3, 2, 1)$, a broader peak has been observed. This is also expected by the present result, since the broad peak around $(3, 2, 1)$ includes larger index of b^* than $(3, 0, 1)$ and b^* shows the largest change from a in $Im\bar{3}$. Therefore, although the splitting of the Bragg peaks has not been found, Pnnm structure will be a candidate to analyze the experimental result.

IV. CONCLUSIONS

Phonon dispersion curves of $RhSb_3$ have been calculated under pressures from 0 GPa to 95 GPa. It is found that the H_7 modes at the H point become unstable above 53 GPa. From Landau theory, the unstable H_7 modes give rise to structural changes into the Pnnm or $R\bar{3}$ structure. Three structures with $Im\bar{3}$, Pnnm, and $R\bar{3}$ symmetry, have been examined under pressures. The Gibbs free energies at 0 K are estimated for these three structures. By comparing each Gibbs free energy, it is found that a first-order transition from $Im\bar{3}$ to Pnnm occurs at around 22 GPa. The transition pressure is close to that observed in the experiment. The present result suggests that the distortions are not self-insertion reaction, but are a collapse of the cage structure. Since the Pnnm structure has larger lattice constant c than the lattice constant of $Im\bar{3}$ structure, some Bragg peaks will appear at a lower angle than the Bragg peak of $Im\bar{3}$ structure, as observed in the experiment. Therefore, it is worth considering the Pnnm structure under pressures.

Acknowledgments

This work was supported by Grants-in-Aid for Scientific Research on Innovative Areas "Heavy Electrons" (No. 20102005) of The Ministry of Education, Culture, Sports, Science, and Technology, Japan, by a Grant-in-Aid for Young Scientists (B) (No. 21740527) of Japan Society for the Promotion of Science, and by N-BARD and IAMR of Hiroshima University.

References

* Electronic address: `hase@hiroshima-u.ac.jp`

[1] M. Udagawa, T. Hasegawa, Y. Takasu, N. Ogita, K. Suekuni, M. A. Avila, T. Takabatake, Y. Ishikawa, N. Takeda, Y. Nemoto, T. Goto, H. Sugawara, D. Kikuchi, H. Sato, C. Sekine, I. Shirotani, J. Yamaura, Y. Nagao, and Z. Hiroi, J. Phys. Soc. Jpn. **77**, Suppl. A, 142 (2008).
[2] Y. Nakai, K. Ishida, H. Sugawara, D. Kikuchi, and H. Sato, Phys. Rev. B **77**, 041101(R) (2008).
[3] S. Tsutsui, H. Kobayashi, J. P. Sutter, H. Uchiyama, A. Q. R. Baron, Y. Yoda, D. Kikuchi, H. Sugawara, C. Sekine, I. Shirotani, A. Ochiai, and H. Sato, J. Phys. Soc. Jpn. **77**, Suppl. A, 257 (2008).
[4] K. Iwasa, M. Kohgi, H. Sugawara, and H. Sato, Physica B **378–380**, 194 (2006).
[5] T. Goto, Y. Nemoto, K. Sakai, T. Yamaguchi, M. Akatsu, T. Yanagisawa, H. Hazama, K. Onuki, H. Sugawara, and H. Sato, Phys. Rev. B **69**, 180511(R) (2004).
[6] G. S. Nolas, D. T. Morelli, and T. M. Tritt, Annu. Rev. Mater. Sci. **29**, 89 (1999).
[7] B. C. Sales, D. Mandrus, B. C. Chakoumakos, V. Keppens, and J. R. Thompson, Phys. Rev. B **56**, 15081 (1997)).
[8] S. Sanda, Y. Aoki, H. Aoki, A. Tsuchiya, D. Kikuchi, H. Sugawara, and H. Sato, J. Phys. Soc. Jpn. **74**, 248 (2005).
[9] T. Hotta, J. Phys. Soc. Jpn. **78**, 073707 (2009).
[10] A. C. Kraemers, M. R. Gallas, J. A. H. da Jornada, and C. A. Perottoni, Phys. Rev. B **75**, 024105 (2007).
[11] A. C. Kraemer, C. A. Perottoni, and J. A. H. da Jornada, Solid State Commun. **133**, 173 (2005).
[12] T. S. Snider, J. V. Badding, S. B. Schujman, and G. A. Slack, Chem. Mater. **12**, 697 (2000).
[13] K. Matsui, J. Hayashi, K. Akahira, K. Ito, K. Takeda, and C. Sekine, J. Phys.: Conf. Ser. **215**, 012005 (2010).
[14] X. Gonze, B. Amadon, P.-M. Anglade, J.-M. Beuken, F. Bottin, P. Boulanger, F. Bruneval,' D. Caliste, R. Caracas, M. Cote, T. Deutsch, L. Genovese, Ph. Ghosez, M. Giantomassi, S. Goedecker, D. R. Hamann, P. Hermet, F. Jollet, G. Jomard, S. Leroux, M. Mancini, S. Mazevet, M. J. T. Oliveira, G. Onida, Y. Pouillon, T. Rangel, G.-M. Rignanese, D. Sangalli, R. Shaltaf, M. Torrent, M. J. Verstraete, G. Zerah, J. W. Zwanziger, Computer Phys. Commun. **180**, 2582 (2009).
[15] X. Gonze, G.-M. Rignanese, M. Verstraete, J.-M. Beuken, Y. Pouillon, R. Caracas, F. Jollet, M. Torrent, G. Zerah, M. Mikami, Ph. Ghosez, M. Veithen, J.-Y. Raty, V. Olevano, F. Bruneval, L. Reining, R. Godby, G. Onida, D. R. Hamann, and D. C. Allan. Zeit. Kristallogr. **220**, 558 (2005).
[16] The ABINIT code is a common project of the Université Catholique de Louvain, Corning Incorporated, and other contributors (URL http://www.abinit.org).
[17] S. Goedecker, SIAM J. on Scientific Computing **18**, 1605 (1997).
[18] M. C. Payne, M. P. Teter, D. C. Allan, T. A. Arias, and J. D. Joannopoulos, Rev. Mod. Phys. **64**, 1045 (1992).
[19] X. Gonze, Phys. Rev. B **54**, 4383 (1996).
[20] J. P. Perdew and Y. Wang, Phys. Rev. B **45**, 13244 (1992).
[21] N. Troullier and J. L. Martins, Phys. Rev. B **43**, 1993 (1991).
[22] M. Fuchs and M. Scheffler, Computer Phys. Commun. **119**, 67 (1999).
[23] H. J. Monkhorst and J. D. Pack, Phys. Rev. B **13**, 5188 (1976).
[24] X. Gonze, Phys. Rev. B **55**, 10337 (1997).
[25] X. Gonze and C. Lee, Phys. Rev. B **55**, 10355 (1997).
[26] F. Birch, Phys. Rev. **71**, 809 (1947).